Inorg. Chem. **2007**, *46*, 9213–9220

Syntheses, Structures, Magnetism, and Optical Properties of Lutetium-Based Interlanthanide Selenides

Geng Bang Jin,[†] Eun Sang Choi,[‡] Robert P. Guertin,[§] James S. Brooks,[‡] Corwin H. Booth,[||] and Thomas E. Albrecht-Schmitt*,[†]

Department of Chemistry and Biochemistry and Center for Actinide Science, Auburn University, Auburn, Alabama 36849, Department of Physics and National High Magnetic Field Laboratory, Florida State University, Tallahassee, Florida 32310, Department of Physics and Astronomy, Tufts University, Medford, Massachusetts 02155, and Chemical Sciences Division, Lawrence Berkeley National Laboratory, 1 Cyclotron Road, Berkeley, California 94720

Received May 24, 2007

Ln_3LuSe_6 (Ln = La, Ce), β-LnLuSe$_3$ (Ln = Pr, Nd), and $Ln_xLu_{4-x}Se_6$ (Ln = Sm, Gd; $x = 1.82$, 1.87) have been synthesized using a Sb_2Se_3 flux at 1000 °C. Ln_3LuSe_6 (Ln = La, Ce) adopts the U_3ScS_6-type three-dimensional structure, which is constructed from two-dimensional $^2_\infty[Ln_3Se_6]^{3-}$ slabs with the gaps between these slabs being filled by octahedrally coordinated Lu^{3+} ions. The series of β-LnLuSe$_3$ (Ln = Pr, Nd) are isotypic with $UFeS_3$. Their structures include layers formed from $LuSe_6$ octahedra that are separated by eight-coordinate Ln^{3+} (Ln = Pr, Nd) ions in bicapped trigonal prismatic environments. $Sm_{1.82}Lu_{2.18}Se_6$ and $Gd_{1.87}Lu_{2.13}Se_6$ crystallize in the disordered F-Ln_2S_3 type structure with the eight-coordinate bicapped trigonal prismatic Ln(1) ions residing in the one-dimensional channels formed by three different double chains via edge- and corner-sharing. These double chains are constructed from Ln(2)Se$_7$ monocapped trigonal prisms, Ln(3)Se$_6$ octahedra, and Ln(4)S$_6$ octahedra, respectively. The magnetic susceptibilities of β-PrLuSe$_3$ and β-NdLuSe$_3$ follow the Curie–Weiss law. $Sm_{1.82}Lu_{2.18}Se_6$ shows van Vleck paramagnetism. Magnetic susceptibility measurements show that $Gd_{1.87}Lu_{2.13}Se_6$ undergoes an antiferromagnetic transition around 4 K. Ce_3LuSe_6 exhibits soft ferromagnetism below 5 K. The optical band gaps for La_3LuSe_6, Ce_3LuSe_6, β-PrLuSe$_3$, β-NdLuSe$_3$, $Sm_{1.82}Lu_{2.18}Se_6$, and $Gd_{1.87}Lu_{2.13}Se_6$ are 1.26, 1.10, 1.56, 1.61, 1.51, and 1.56 eV, respectively.

Introduction

Interlanthanide chalcogenides have been the focus of intense interest because of their remarkably complex structures, potentially tunable optical properties, and in some cases, atypical magnetism.[1−22] One of the primary goals in this work is to obtain phases where the different lanthanide ions are present in the crystalline lattice in an ordered arrangement. There are several methods for achieving this goal including the selection of lanthanides from opposite ends

* To whom correspondence should be addressed. E-mail: albreth@auburn.edu. Fax: 334-844-6959.
[†] Auburn University.
[‡] Florida State University.
[§] Tufts University.
[||] Lawrence Berkeley National Laboratory.

(1) Moreau, J. M. *Mater. Res. Bull.* **1968**, *3*, 427.
(2) Moreau, J. M.; Mareschal, J.; Bertaut, E. F. *Solid State Commun.* **1968**, *6*, 751.
(3) Mareschal, J.; Moreau, J. M.; Ollivier, G.; Pataud, P.; Sivardiere, J. *Solid State Commun.* **1969**, *7*, 669.
(4) Rodier, N.; Laruelle, P. *C. R. Seances Acad. Sci. Ser. C* **1970**, *270*, 2127.
(5) Coutures, J.; Coutures, J. P. *J. Solid State Chem.* **1976**, *19*, 29.
(6) Müller-Buschbaum, H.; Graebner, P. -H. *Z. Anorg. Allg. Chem.* **1971**, *386*, 158.
(7) Ijdo, D. J. W. *Acta Crystallogr. B* **1980**, *36*, 2403.
(8) Ito, K.; Tezuka, K.; Hinatsu, Y. *J. Solid State Chem.* **2001**, *157*, 173.
(9) Deepa, M.; Varadaraju, U. V. *Mater. Res. Soc. Symp. Proc.* **1998**, *527*, 507.
(10) Berndt, U.; Maier, D.; Keller, C. *J. Solid State Chem.* **1976**, *16*, 189.
(11) Ito, K.; Tezuka, K.; Hinatsu, Y. *J. Solid State Chem.* **2001**, *157*, 173.
(12) Rodier, N.; Julien, R.; Tien, V. *Acta Crystallogr. C* **1983**, *39*, 670.
(13) Carre, D.; Laruelle, P. *Acta Crystallogr. B* **1974**, *30*, 952.
(14) Mitchell, K.; Somers, R. C.; Huang, F. Q.; Ibers, J. A. *J. Solid State Chem.* **2004**, *177*, 709.
(15) Jin, G. B.; Choi, E. S.; Guertin, R. P.; Brooks, J. S.; Bray, T. H.; Booth, C. H.; Albrecht-Schmitt, T. E. *Chem. Mater.* **2007**, *19*, 567.
(16) Rodier, N.; Tien, V. *C. R. Seances Acad. Sci. Ser. C* **1974**, *279*, 817.
(17) Rodier, N.; Firor, R. L.; Tien, V.; Guittard, M. *Mater. Res. Bull.* **1976**, *11*, 1209.
(18) Rodier, N. *Bull. Soc. Fr. Mineral. Cristallogr.* **1973**, *96*, 350.
(19) Carré, D.; Laruelle, P. *Acta Crystallogr. B* **1973**, *29*, 70.
(20) Gray, D. L.; Rodriguez, B. A.; Chan, G. H.; Van Duyne, R. P.; Ibers, J. A. *J. Solid State Chem.* **2007**, *180*, 1527.

10.1021/ic701012j CCC: $37.00 © 2007 American Chemical Society
Published on Web 10/03/2007

of the series in an attempt to capitalize on the marked difference in size of the early versus late lanthanide ions. Therefore, ternary interlanthanide chalcogenides usually include one larger ion (Ln) and one smaller ion (Ln′) that are from opposite ends of lanthanide series with different coordination environments to avoid possible disordering. Early lanthanides, such as La^{3+} and Ce^{3+}, are often found in eight- and nine-coordinate environments, whereas late lanthanides (e.g., Yb^{3+} and Lu^{3+}) are usually found in six- and seven-coordinate environments. To this end, Ln/Yb/Q (Q = S, Se) phases have been extensively studied. This group is represented by α-$LaYbS_3$[12] ($GdFeO_3$ type),[23] β-$LnYbQ_3$ (Q = S, Se)[12−14] ($UFeS_3$ type),[24] γ-$LnYbS_3$ (Ln = La, Ce),[15] and $LnYb_3S_6$[16,17] (F-Ln_2S_3 type).[25,26]

Er- and Tm-containing ternary compounds have also been prepared, and a number of well-characterized examples exist including $CeTmS_3$,[18] $La_{10}Er_9S_{27}$,[19] γ-LnLn′S_3 (Ln = La, Ce; Ln′ = Er, Tm),[15] $SmEr_3Q_6$ (Q = S, Se)[20] (F-Ln_2S_3 type),[25,26] and $Sm_{0.88}Er_{1.12}Se_3$[20] (U_2S_3 type).[27] Both Er^{3+} and Tm^{3+} ions are paramagnetic. In contrast, the Ln/Lu/Q phases have potentially simpler magnetism because there is at most one paramagnetic ion owing to the $4f^{14}$ configuration of Lu^{3+}.

Recently, we reported the synthesis and characterization of the interlanthanide sulfides δ-$Ln_{2-x}Lu_xS_3$ (Ln = Ce, Pr, Nd).[21] These compounds crystallize in the disordered $CeTmS_3$ structure-type and have band gaps that are dependent on the choice of the lanthanide ion. The magnetic behavior of most lanthanide compounds is complicated, in part, because of substantial crystal-field effects. The δ-$Ln_{2-x}Lu_xS_3$ (Ln = Ce, Pr, Nd) are no exception to this, and δ-$Ce_{1.30}Lu_{0.70}S_3$ deviates from the Curie−Weiss law at low temperatures, a feature that can be ascribed to crystal-field effects. In this present study, we attempt to address the structural and electronic behavior of both ordered and disordered ternary lanthanide lutetium selenides. We disclose the syntheses, structures, optical, and magnetic properties of Ln_3LuSe_6 (Ln = La, Ce), β-$LnLuSe_3$ (Ln = Pr, Nd), and $Ln_xLu_{4-x}Se_6$ (Ln = Sm, Gd; $x = 1.82, 1.87$).

Experimental Section

Starting Materials. La (99.9%, Alfa-Aesar), Ce (99.9%, Alfa-Aesar), Pr (99.9%, Alfa-Aesar), Nd (99.9%, Alfa-Aesar), Sm (99.9%, Alfa-Aesar), Gd (99.9%, Alfa-Aesar), Lu (99.9%, Alfa-Aesar), Se (99.5%, Alfa-Aesar), and Sb (99.5%, Alfa-Aesar) were used as received. The Sb_2Se_3 flux was prepared from the direct reaction of the elements in sealed fused-silica ampules at 850 °C.

Syntheses. Ln_3LuSe_6 (Ln = La, Ce) were synthesized from a reaction of 150 mg of stoichiometric Ln, Lu, and Se and 100 mg of Sb_2Se_3. For β-$LnLuSe_3$ (Ln = Pr, Nd) and $Ln_xLu_{4-x}Se_6$ (Ln = Sm, Gd; $x = 1.82, 1.87$), the reaction mixtures include 150 mg of Ln, Lu, and Se in a molar ratio of 1:1:3 and 100 mg of Sb_2Se_3. All of these starting materials were loaded into fused-silica ampules under an argon atmosphere in a glovebox. The ampules were flame-sealed under vacuum and heated in programmable tube furnaces. The following heating profile was used for all reactions: 2 °C min^{-1} to 500 °C (held for 1 h), 0.5 °C min^{-1} to 1000 °C (held for 14 days), 0.04 °C min^{-1} to 550 °C (held for 2 days), and 0.5 °C min^{-1} to 24 °C. The major title products were found as large black chunks that were well separated from the Sb_2Se_3 flux. The separation of the flux from the products is achieved by slightly tilting the furnaces, which causes the flux to settle to the bottom of the ampules leaving the desired product higher up, making manual separation with the aid of a stereomicroscope trivial. The reaction ampules are located toward the back of the tube furnace, and the flux settles in the farthest and presumably coolest region of the furnace. Once the products were isolated, they were ground for powder X-ray diffraction measurements, which were used to confirm phase purity by comparison of the powder patterns calculated from the single-crystal X-ray structures with the experimental data. Semiquantitative SEM/EDX analyses were performed on several single crystals for each compound using a JEOL 840/Link Isis or JEOL JSM-7000F instruments. Ln, Lu, and Se percentages were calibrated against standards. Sb was not detected in the crystals. The Ln/Lu/Se ratios for Ln_3LuSe_6 (Ln = La, Ce) were determined to be approximately 3:1:6 from EDX analyses, while the ratios of Ln/Lu/Se were close to 1:1:3 for β-$LnLuSe_3$ (Ln = Pr, Nd) and $Ln_xLu_{4-x}Se_6$ (Ln = Sm, Gd; $x = 1.82, 1.87$).

Crystallographic Studies. Single crystals of $Ln_xLu_ySe_z$ (Ln = La, Ce, Pr, Nd, Sm, Gd) were mounted on glass fibers with epoxy and optically aligned on a Bruker APEX single crystal X-ray diffractometer using a digital camera. Initial intensity measurements were performed using graphite-monochromated Mo Kα (λ = 0.71073 Å) radiation from a sealed tube and monocapillary collimator. SMART (version 5.624) was used for preliminary determination of the cell constants and data collection control. The intensities of reflections of a sphere were collected by a combination of three sets of exposures (frames). Each set had a different ϕ angle for the crystal, and each exposure covered a range of 0.3° in ω. A total of 1800 frames were collected with exposure times per frame of 10 or 20 s depending on the crystal.

For $Ln_xLu_ySe_z$ (Ln = La, Ce, Pr, Nd, Sm, Gd), determination of integrated intensities and global refinement were performed with the Bruker SAINT (version 6.02) software package using a narrow-frame integration algorithm. These data were treated first with a face-indexed numerical absorption correction using XPREP,[28] followed by a semiempirical absorption correction using SADABS.[29] The program suite SHELXTL (version 6.12) was used for space group determination (XPREP), direct methods structure solution (XS), and least-squares refinement (XL).[28] The final refinements included anisotropic displacement parameters for all atoms and secondary extinction. Some crystallographic details are given in Table 1. Additional crystallographic information can be found in the Supporting Information.

The structures of Ln_3LuSe_6 (Ln = La, Ce) and β-$LnLuSe_3$ (Ln = Pr, Nd) are ordered. For these compounds, the assignments of the cation positions were straightforward. $Ln_xLu_{4-x}Se_6$ (Ln = Sm,

(21) Jin, G. B.; Choi, E. S.; Guertin, R. P.; Brooks, J. S.; Bray, T. H.; Booth, C. H.; Albrecht-Schmitt, T. E. *J. Solid State Chem.* **2007**, in press.
(22) Jin, G. B.; Choi, E. S.; Guertin, R. P.; Brooks, J. S.; Bray, T. H.; Booth, C. H.; Albrecht-Schmitt, T. E. *J. Solid State Chem.* **2007**, in press.
(23) Marezio, M.; Remeika, J. P.; Dernier, P. D. *Acta Crystallogr. B* **1970**, *26*, 2008.
(24) Noel, H.; Padiou, J. *Acta Crystallogr. B* **1976**, *32*, 1593.
(25) Schleid, T.; Lissner, F. *J. Alloys Compds.* **1992**, *189*, 69.
(26) Fang, C. M.; Meetsma, A.; Wiegers, G. A. *J. Alloys Compds.* **1993**, *201*, 255.
(27) Zachariasen, W. H. *Acta Crystallogr.* **1949**, *2*, 291.
(28) Sheldrick, G. M. *SHELXTL PC, An Integrated System for Solving, Refining, and Displaying Crystal Structures from Diffraction Data*, version 6.12; Siemens Analytical X-Ray Instruments, Inc.: Madison, WI, 2001.
(29) Sheldrick, G. M. *Acta Crystallogr. A* **1995**, *51*, 33.

Table 1. Crystallographic Data for $Ln_xLu_ySe_z$ (Ln = La, Ce, Pr, Nd, Sm, Gd)

formula	La_3LuSe_6	Ce_3LuSe_6	β-$PrLuSe_3$	β-$NdLuSe_3$	$Sm_{1.82}Lu_{2.18}Se_6$	$Gd_{1.87}Lu_{2.13}Se_6$
fw	1065.46	1069.09	552.76	556.09	1128.83	1140.50
color	black	black	black	black	black	black
cryst syst	orthorhombic	orthorhombic	orthorhombic	orthorhombic	monoclinic	monoclinic
space group	*Pnnm* (No. 58)	*Pnnm* (No. 58)	*Cmcm* (No. 63)	*Cmcm* (No. 63)	$P2_1/m$ (No. 11)	$P2_1/m$ (No. 11)
a (Å)	14.6195(10)	14.5020(9)	4.0052(10)	3.9946(5)	11.3925(13)	11.4274(12)
b (Å)	17.5736(12)	17.4954(11)	12.996(3)	13.0015(17)	4.0483(5)	4.0542(4)
c (Å)	4.1542(3)	4.1129(3)	9.865(3)	9.8583(13)	11.6844(14)	11.7160(12)
β (deg)					108.915(2)	109.005(2)
V (Å^3)	1067.29(13)	1043.52(12)	513.5(2)	512.00(11)	509.79(11)	513.20(9)
Z	4	4	4	4	2	2
T (K)	193	193	193	193	193	193
λ (Å)	0.71073	0.71073	0.71073	0.71073	0.71073	0.71073
ρ_{calcd} (g cm^{-3})	6.631	6.805	7.150	7.214	7.354	7.381
μ (cm^{-1})	413.24	430.70	495.66	503.36	525.94	534.34
$R(F)^a$	0.0273	0.0212	0.0429	0.0226	0.0300	0.0308
$R_w(F_o^2)^b$	0.0645	0.0485	0.1049	0.0601	0.0822	0.0817

^{a} $R(F) = \sum||F_o| - |F_c||/\sum|F_o|$ for $F_o^2 > 2\sigma(F_o^2)$. ^{b} $R_w(F_o^2) = [\sum[w(F_o^2 - F_c^2)^2]/\sum wF_o^4]^{1/2}$.

Table 2. Ternary Interlanthanide Sulfides Prepared Using Sb_2S_3 Flux at 1000 °C[a]

	Eu^{2+}	La^{3+}	Ce^{3+}	Pr^{3+}	Nd^{3+}	Sm^{3+}	Gd^{3+}
Tb^{3+}	●						
Dy^{3+}	●	♦ △					
Ho^{3+}	●	♦ △	◇				
Er^{3+}	●	♦	♦				
Tm^{3+}	●	♦	♦	△			
Yb^{3+}	●	♦	♦	△	△	△	△
Lu^{3+}	●	△	◇	◇	◇	△	

[a] Ordered structure types: ▲ β-$LnLn'S_3$,[12−14] ♦ γ- $LnLn'S_3$,[15] ■ U_3ScS_6,[32] ● $CaFe_2O_4$.[33] Disordered structure types: △ F-Ln_2S_3,[25,26] ◇ δ-$LnLn'S_3$,[18,21] □ U_2S_3,[27] ○ Y_5S_7.[34]

Table 3. Ternary Interlanthanide Selenides Prepared Using Sb_2Se_3 Flux at 1000 °C[a]

	Eu^{2+}	La^{3+}	Ce^{3+}	Pr^{3+}	Nd^{3+}	Sm^{3+}	Gd^{3+}
Tb^{3+}	●	□					
Dy^{3+}	●		□				
Ho^{3+}	●						
Er^{3+}	●	◇			△		
Tm^{3+}	●	△	△	△	△	△	△
Yb^{3+}	●	○	▲	▲	▲	△	△
Lu^{3+}	●	■	■	▲	▲	△	△

[a] Ordered structure types: ▲ β-$LnLn'S_3$,[12−14] ♦ γ- $LnLn'S_3$,[15] ■ U_3ScS_6,[32] ● $CaFe_2O_4$.[33] Disordered structure types: △ F-Ln_2S_3,[25,26] ◇ δ-$LnLn'S_3$,[18,21] □ U_2S_3,[27] ○ Y_5S_7.[34]

Gd; $x = 1.82, 1.87$) compounds crystallize in the F-Ln_2S_3[25,26] type structure, which is highly disordered. All four cation sites, including one eight-coordinate position (Ln(1)), one seven-coordinate position (Ln(2)), and two octahedral positions (Ln(3) and Ln(4)), were assumed to be occupied by both metals at the beginning of the refinements. The final refinements showed that the occupancies of Lu atoms in Ln(1), Ln(2), Ln(3), and Ln(4) positions are 0.02, 0.32, 0.88, and 0.95, respectively, for the Sm-based compound and 0.04, 0.40, 0.84, and 0.86 for Gd case. These results gave rise to the formula of $Sm_{1.82}Lu_{2.18}Se_6$ and $Gd_{1.87}Lu_{2.13}Se_6$, which are consistent with the 1:1:3 ratios from EDX analysis. It is worth noting that $Gd_{1.87}Lu_{2.13}Se_6$ has a higher degree of disorder than $Sm_{1.82}Lu_{2.18}Se_6$ because of the decrease in the difference in the size of the cations, even though they have similar Ln/Lu ratios.

Powder X-ray Diffraction. Powder X-ray diffraction patterns were collected with a Rigaku Miniflex powder X-ray diffractometer using Cu Kα ($\lambda = 1.54056$ Å) radiation.

Magnetic Susceptibility Measurements. Magnetic susceptibility data were collected from powders in gelcap sample holders with a Quantum Design MPMS 7T magnetometer/susceptometer between 2 and 300 K and in applied fields up to 7 T. DC susceptibility measurements were made under zero-field-cooled conditions with an applied field of 0.1 T. Magnetic susceptibility for Ce_3LuSe_6 under zero-field-cooled (ZFC) and field-cooled (FC) conditions were measured with 0.01 T applied field between 2 and 25 K. Susceptibility values were corrected for the sample diamagnetic contribution according to Pascal's constants,[30] as well as for the sample holder diamagnetism. Experimental effective magnetic moments and Weiss constants for Ce_3LuSe_6, β-$PrLuSe_3$, β-$NdLuSe_3$, and $Gd_{1.87}Lu_{2.13}Se_6$ were obtained from extrapolations from fits between 100 and 300 K.

UV−vis-NIR Diffuse Reflectance Spectroscopy. The diffuse reflectance spectra for $Ln_xLu_ySe_z$ (Ln = La, Ce, Pr, Nd, Sm, Gd) were measured from 200 to 2500 nm using a Shimadzu UV3100 spectrophotometer equipped with an integrating sphere attachment. The Kubelka−Munk function was used to convert diffuse reflectance data to absorption spectra.[31]

Results and Discussion

Synthesis of Ln/Ln′/Q using Sb_2Q_3 Fluxes (Q = S, Se). There are a large number of synthetic parameters that significantly affect the type of interlanthanide chalcogenide obtained in flux-based reactions. These parameters include the choice of flux, reaction temperature, stoichiometry, and choices of lanthanides and chalcogens. It has been shown that temperature changes as small as 50 K (1173 K vs 1123 K) can induce changes in product formation.[20] In our work, we have focused on the use of Sb_2Q_3 (Q = S, Se) fluxes to prepare ternary and quaternary interlanthanide chalcogenides.[15,21,22] Eight different structure types have been identified for ternary interlanthanide chalcogenides prepared with these fluxes at 1273 K.[12−15,18,21,25−27,32−34] These compounds are given in Tables 2 and 3. A change of the flux from KI to Sb_2Q_3 (Q = S, Se) produces different compounds. For example, when La, Yb, and S are reacted in a KI flux at

(30) Mulay, L. N.; Boudreaux, E. A. *Theory and Applications of Molecular Diamagnetism*; Wiley-Interscience: New York, 1976.
(31) Wendlandt, W. W.; Hecht, H. G. *Reflectance Spectroscopy*; Interscience Publishers: New York, 1966.
(32) Rodier, N.; Tien, V. *Acta Crystallogr.* **1976**, *32*, 2705.
(33) Becker, D. F.; Kasper, J. S. *Acta Crystallogr.* **1957**, *10*, 332.
(34) Adolphe, C. *Ann. Chim. (Paris)* **1965**, *10*, 271.

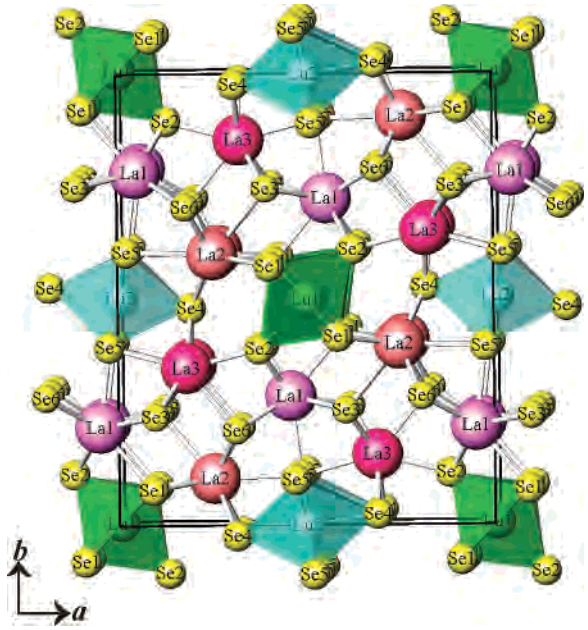

Figure 1. Illustration of the three-dimensional structure of La_3LuSe_6 viewed down the *c*-axis.

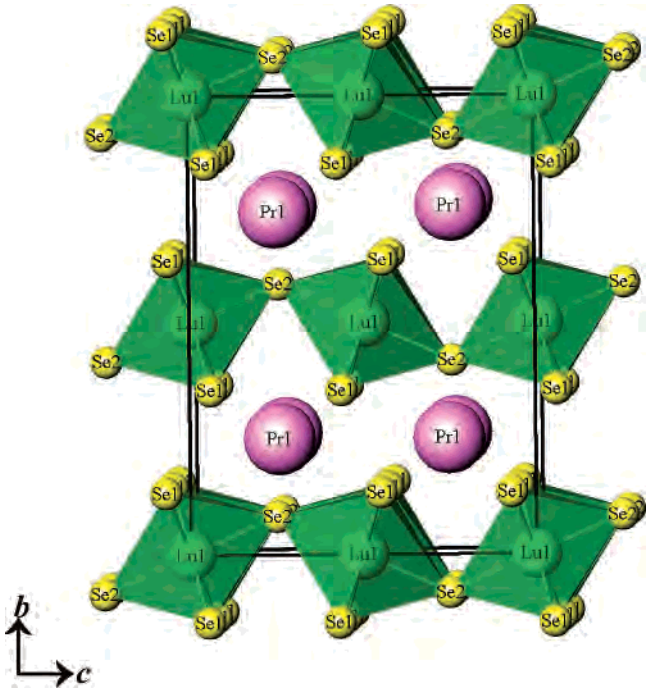

Figure 2. Unit cell of β-$PrLuSe_3$ viewed along the *a*-axis. Pr−Se bonds have been omitted for clarity.

1123 K, β-$LaYbS_3$ is obtained.[14] In contrast, when the same reaction is performed using a Sb_2S_3 flux, γ-$LaYbS_3$ crystallizes. We have not noted the same temperature sensitivity as observed for the halide fluxes and find instead that temperature primarily affects crystal growth.

The structures of Ln/Ln′/Q phases depend highly on the choices of Ln and Ln′. This is especially true for La/Ln′/Se, which can adopt five different structures with the variation of Ln′. Ordered phases predominate when Ln and Ln′ ions have larger differences in size. Disordered compounds are often present when the difference in size of the lanthanide ions becomes too small because of the similar structural chemistry of lanthanides; some exceptions to this include $LaLu_3S_6$ and $La_xYb_{5-x}Se_7$. The limitations of using Sb_2Q_3 (Q = S, Se) fluxes to prepare LnLn′Q include: (1) Attempts to prepare interlanthanide tellurides have not succeeded. (2) When the ionic radii of the two Ln^{3+} ions approach equality, the product fails to separate from the flux, and the resultant microcrystalline compounds do not diffract well. (3) Occasionally, the use of a stereomicroscope to distinguish and manually separate products from Sb_2Q_3 (*Q* = S, Se) fluxes is difficult to accomplish. While this was not the case for this or previously published works, not all reactions yield crystals well separated from the flux. We have not found a good solvent or acid for dissolving the flux that leaves the product unreacted.

Structures of $Ln_xLu_ySe_z$ (Ln = La, Ce, Pr, Nd, Sm, Gd). The Ln_3LuSe_6 (Ln = La, Ce) compounds adopt the U_3ScS_6-type[32] structure. The unit cell of La_3LuSe_6, projected along the *c*-axis, is shown in Figure 1. There are three crystallographically unique Ln sites (4*g*) and two octahedral Lu positions (2*d*, 2*b*) in the structure. Both Ln(1) and Ln(2) atoms are surrounded by eight Se atoms and occur as bicapped trigonal prisms. Ln(3) sites are seven-coordinate in a monocapped trigonal prismatic environment. $LnSe_8$ and $LnSe_7$ polyhedra share faces or edges with each other to form two-dimensional slabs extending in the [*ac*] plane. Furthermore, these slabs connect at the Se(4) positions to produce a three-dimensional structure. The gaps between these slabs are filled by isolated one-dimensional edge-sharing $LuSe_6$ octahedral chains running down the *c*-axis. The bond distances for these two compounds, which can be found in Supporting Information, are normal compared to average values reported by Shannon.[35] In the case of La_3LuSe_6, the bond distances for the $LaSe_8$, $LaSe_7$, and $LuSe_6$ polyhedra range from 2.9982(8) to 3.3408(11), 2.9229(11) to 3.1116(11), and 2.6629(9) to 2.8257(6) Å, respectively.

The series of β-$LnLuSe_3$ (Ln = Pr, Nd) are isotypic with $UFeS_3$.[24] The structure, as shown in Figure 2, is constructed from two-dimensional $LuSe_6$ octahedra layers, which are separated by Ln^{3+} ions. The Pr^{3+} and Nd^{3+} coordinate to eight Se atoms with a bicapped trigonal prismatic geometry. The connectivities within $LuSe_6$ layers are illustrated in Figure 3. The $LuSe_6$ octahedral units are edge-sharing along the *a*-axis and corner-sharing along the *c*-axis. The bond lengths within these two compounds are regular. For example, the Pr−Se and Lu−Se distances in compound β-$PrLuSe_3$ are in the range of 2.9035(18) and 3.3670(17) and 2.7102(10) and 2.8072(11) Å, respectively.

$Sm_{1.82}Lu_{2.18}Se_6$ and $Gd_{1.87}Lu_{2.13}Se_6$ crystallize in F-Ln_2S_3-type[25,26] structure, which was detailed in one of our previous papers.[22] As shown in Figure 4, the eight-coordinate bicapped trigonal prismatic Ln(1) ions (Figure 5) sit in the one-dimensional channels formed by three different double chains via edge- and corner-sharing. These double chains, which all run down the *b*-axis, are constructed from $Ln(2)Se_7$

(35) Shannon, R. D. *Acta Crystallogr. A* **1976**, *32*, 751.
(36) Kittel, C. *Introduction to Solid State Physics*, 6th ed.; Wiley, New York, 1986.

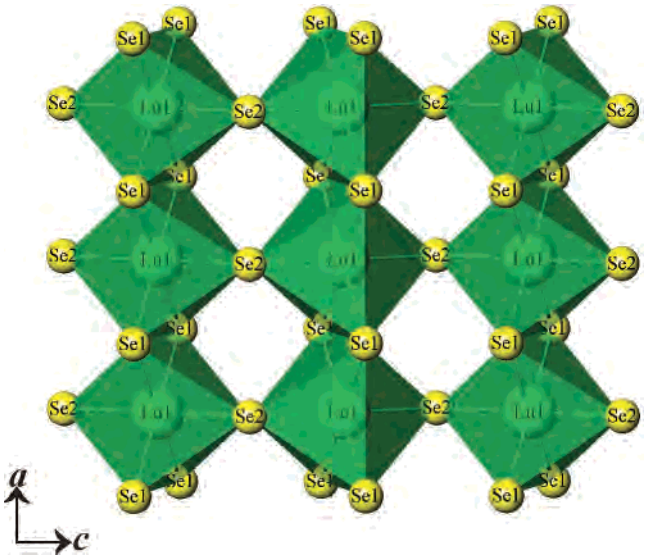

Figure 3. Depiction of an individual $LuSe_6$ octahedra layer viewed down the *b*-axis in β-$PrLuSe_3$.

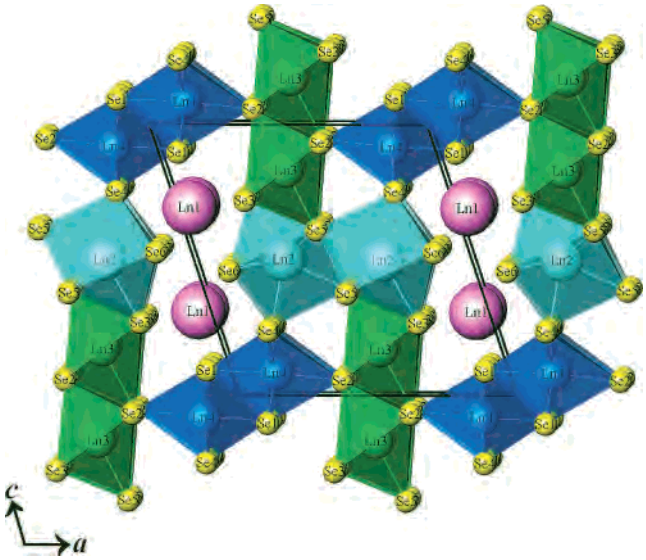

Figure 4. View of the three-dimensional channel structure of $Sm_{1.82}Lu_{2.18}Se_6$ along the *b*-axis.

monocapped trigonal prisms, $Ln(3)Se_6$ octahedra, and $Ln(4)S_6$ octahedra, respectively. Within each double chain, the building polyhedra share edges with each other both in the direction of chain propagation and with adjacent chains. For $Sm_{1.82}Lu_{2.18}Se_6$, the average distances for $Ln(1)S_8$, $Ln(2)Se_7$, $Ln(3)Se_6$,and $Ln(4)Se_6$ polyhedra are 3.0406(10), 2.9230(10), 2.8064(10), and 2.7791(9) Å, respectively, which are comparable to Shannon's data:[35] 3.05 Å for $SmSe_8$, 3.00 Å for $SmSe_7$, 2.90 Å for $LuSe_7$, and 2.84 Å for $LuSe_6$.

Magnetic Susceptibility Measurements. Figure 6 shows the temperature dependence of the inverse molar magnetic susceptibilities for β-$LnLuSe_3$ (Ln = Pr, Nd). Both compounds are paramagnetic and deviate from the Curie−Weiss law below 40 K. The effective magnetic moment and Weiss constant were obtained by fitting the high-temperature susceptibility data into the Curie−Weiss law. As shown in Table 4, the effective magnetic moments are close to

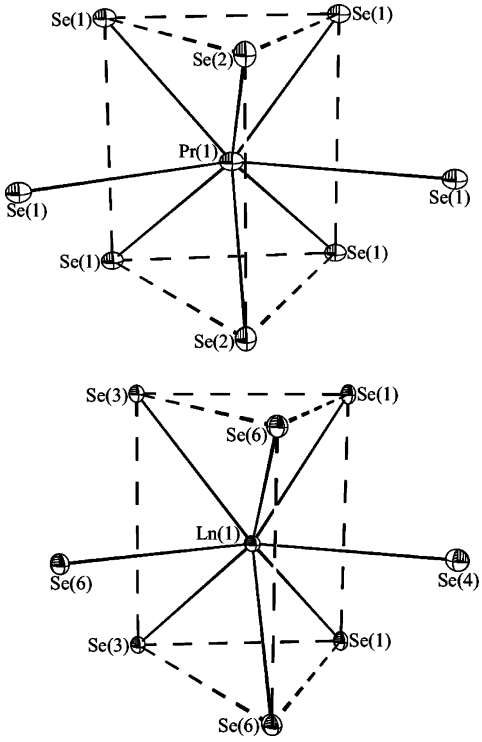

Figure 5. Illustrations of the coordination environments for Pr ions in β-$PrLuSe_3$ and Sm(1)/Lu(1) ions in $Sm_{1.82}Lu_{2.18}Se$.

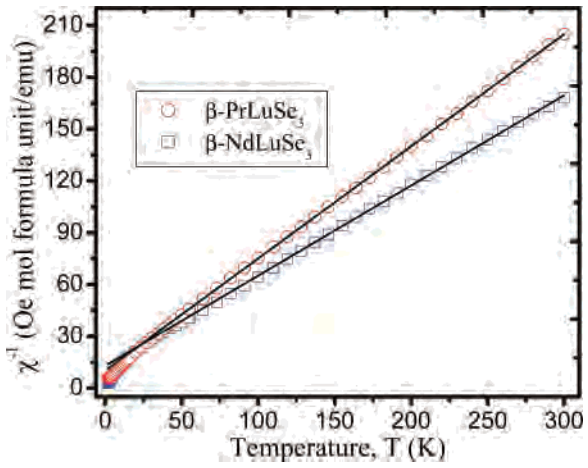

Figure 6. Temperature dependence of the reciprocal molar magnetic susceptibility for β-$PrLuSe_3$ and β-$NdLuSe_3$, under an applied magnetic field of 0.1 T between 2 and 300 K. The straight line represents the fit to Curie−Weiss law in the range of 100−300 K.

calculated values for free Ln^{3+} ions. The negative θ_p values indicate antiferromagnetic coupling between magnetic ions.

The magnetic susceptibility of $Sm_{1.82}Lu_{2.18}Se_6$ shows van Vleck paramagnetic behavior similar to the Sm metal, which is displayed in Figure 7. There is no magnetic transition down to 2 K, and the susceptibility data do not follow the Curie−Weiss law. The difference between the ground state ($^6H_{5/2}$) and the first excited state ($^6H_{7/2}$) of Sm^{3+} is not large compared to thermal energy (k_BT). Therefore, the excited states make significant contributions to the magnetic susceptibility at high temperature.[37] The experimental effective magnetic moment of Sm^{3+} can be determined approximately

Table 4. Magnetic Parameters for Ce_3LuSe_6, β-$LnLuSe_3$ (Ln = Pr, Nd), and $Gd_{1.87}Lu_{2.13}Se_6$

formula	P_{cal} (μ_B)	P_{eff} (μ_B)	θ_p (K)	R^2
Ce_3LuSe_6	4.40	4.56(1)	−20(1)	0.99959
β-$PrLuSe_3$	3.58	3.509(3)	−15.6(4)	0.99993
β-$NdLuSe_3$	3.62	3.913(9)	−25(1)	0.99961
$Gd_{1.87}Lu_{2.13}Se_6$	10.86	11.77(1)	−4.4(4)	0.99991

[a] P_{cal} and P_{eff}: calculated[36] and experimental, respectively, effective magnetic moments per formula unit. [b] Weiss constant (θ_p) and goodness of fit (R^2) obtained from high-temperature (100−300 K) data.

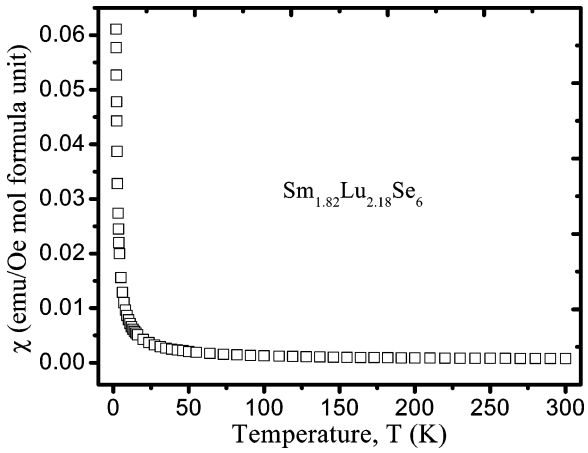

Figure 7. Molar magnetic susceptibility vs temperature between 2 and 300 K for $Sm_{1.82}Lu_{2.18}Se_6$. Data were taken under an applied magnetic field of 0.1 T.

using $\mu_{eff} = [3k_B\chi_m T/(L\mu_0\mu_B^2)]^{1/2}$, where k_B is Boltzmann constant, L is Avogadro's number, μ_0 is vacuum permeability, T is temperature (K), and χ_m is molar susceptibility. At T = 300 K, μ_{eff} = 1.02 μ_B, which is smaller than the calculated value (1.55 μ_B) for free Sm^{3+} ions using the van Vleck formula.[37] This is probably caused by crystal-field effects. $Sm_{1.82}Lu_{2.18}Se_6$ is an excellent example of the usefulness of incorporating a diamagnetic lanthanide into interlanthanide selenides. If another paramagnetic lanthanide been selected, as was done for Er_3SmSe_6,[20] the van Vleck behavior of Sm^{3+} might have been masked. This is especially pronounced for Sm^{3+} because it has the smallest measured moment for a lanthanide.

The magnetic susceptibility of $Gd_{1.87}Lu_{2.13}Se_6$ obeys the Curie−Weiss law above the temperature ∼4 K where it undergoes a sharp antiferromagnetic transition, as shown in Figure 8. The effective magnetic moment and Weiss constant were obtained to be 11.77(1) μ_B per formula unit and −4.4(4) K. The magnetization measurement was performed at 2 K, and the results are presented in Figure 9. The saturation moment per Gd^{3+} ion is 7.5 μ_B, which is close to the value for the free Gd^{3+} ion (7.94 μ_B) assuming g = 2. There is a weak spin reorientation transition at approximately H = 0.5 T.

Ce_3LuSe_6 shows a deviation from the Curie−Weiss law near 70 K caused by crystal-field effects. A magnetic transition was observed below 5 K, which is illustrated in Figure 10. A small divergence on the ZFC-FC measurements

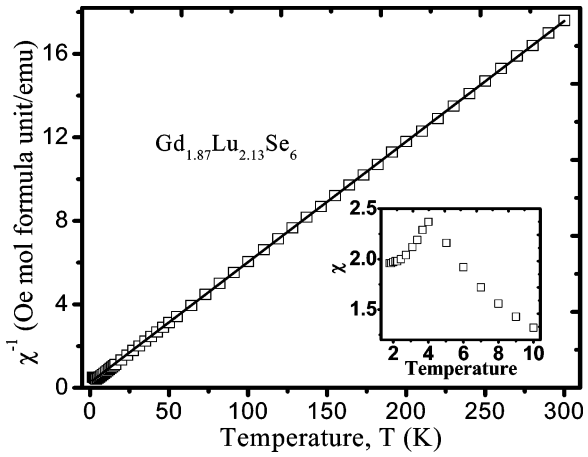

Figure 8. Inverse molar magnetic susceptibility vs temperature for $Gd_{1.87}Lu_{2.13}Se_6$ under an applied magnetic field of 0.1 T between 2 and 300 K. The solid line represents the fit to Curie−Weiss law in the range of 100−300 K. Inset shows the molar magnetic susceptibility at low temperature.

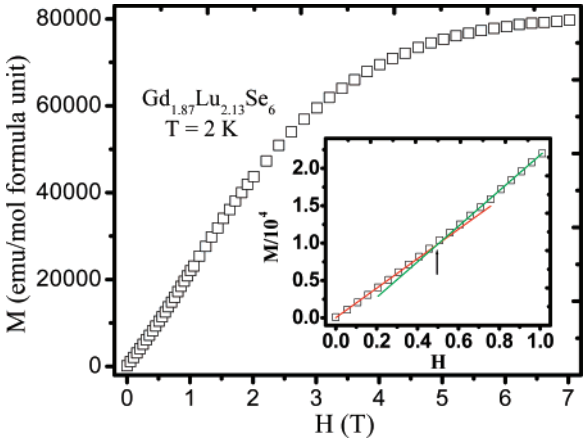

Figure 9. Magnetization for $Gd_{1.87}Lu_{2.13}Se_6$ as a function of applied field at 2 K. Inset shows the $M(H)$ curve between 0 and 1 T. Red and green lines are linear fits extended from zero field and from 1 T, respectively. Slight increasing of the slope and the weak spin reorientation transition field at the junction (up arrow) can be observed.

(Figure 11) below this temperature may indicate a ferromagnetic component of the transition or might be caused by small temperature fluctuations. To investigate the magnetic transition in detail, the magnetization measurements at 2 K were conducted as well. Figure 12 shows the field-dependent magnetizations for Ce_3LuSe_6. $M(H)$ increases abruptly at low field, which is consistent with ferromagnetic behavior. However, the lack of substantial difference between the ZFC and FC measurements, as well as the absence of magnetic hysteresis at 2 K, is indicative of soft ferromagnet behavior.[38] The saturation moment per Ce^{3+} ion (1.13 μ_B) is substantially smaller than the moment for the free Ce^{3+} ion (2.54 μ_B), assuming g = 6/7. This can probably be ascribed to crystal-field splitting of the ground state of the Ce^{3+} ion ($^2F_{5/2}$). The Weiss constant from the fit of the data from 100 to 300 K for Ce_3LuSe_6 was determined to be −20(1) K, indicating antiferromagnetic interactions between Ce^{3+} ions at higher temperatures. It is worth noting that the $|\theta_p|$ value may be enlarged because of the crystal-field splitting of the

(37) Van Vleck, J. H. *The Theory of Electric and Magnetic Susceptibilities*; Oxford University Press: London, 1932.

(38) Singh, S.; Sheet, G.; Raychaudhuri, P.; Dhar, S. K. *Appl. Phys. Lett.* **2006**, *88*, 022506.

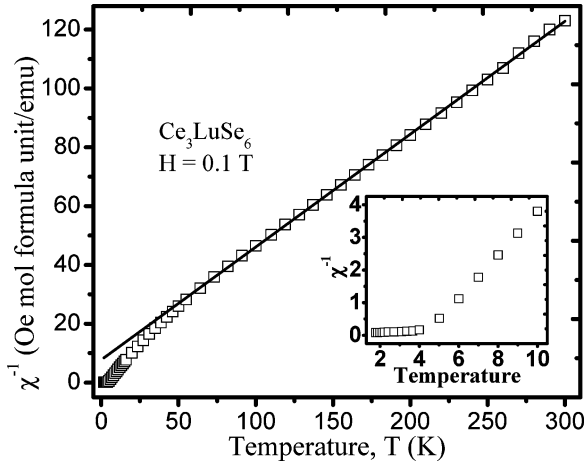

Figure 10. Inverse molar magnetic susceptibility as a function of temperature for Ce_3LuSe_6 under an applied magnetic field of 0.1 T between 2 and 300 K. The straight line represents the fit to Curie−Weiss law in the range of 100−300 K. Inset shows the inverse molar magnetic susceptibility at low temperature.

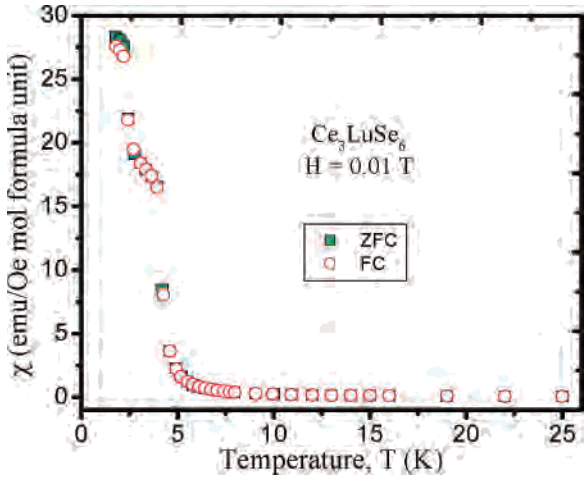

Figure 11. Molar magnetic susceptibility as a function of temperature for Ce_3LuSe_6 under ZFC and FC conditions with an applied magnetic field of 0.01 T between 2 and 25 K.

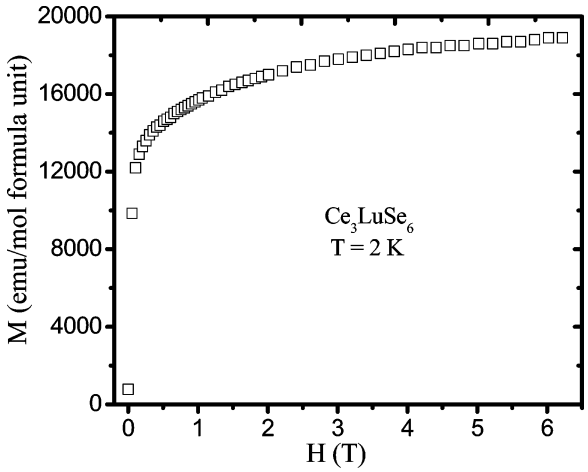

Figure 12. Magnetization for Ce_3LuSe_6 as a function of applied field at 2 K.

full $J = 5/2$ multiplet for Ce^{3+}. To conclude, Ce_3LuSe_6 orders ferromagnetically with a weak antiferromagnetic component that might be the result of canted spins of Ce^{3+}.

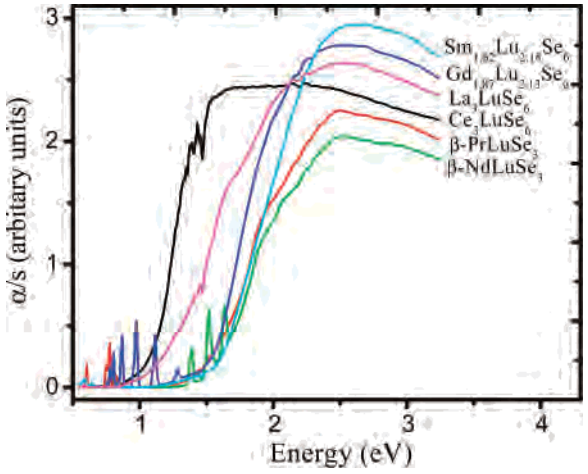

Figure 13. UV−vis diffuse reflectance spectra of $Ln_xLu_ySe_z$ (Ln = La, Ce, Pr, Nd, Sm, Gd).

Optical Properties. There are few interlanthanide selenides reported in the literature. $SmEr_3Se_6$, a red compound, was determined to be a wide direct band gap semiconductor with a band gap of 2.0 eV.[20] The series of compounds, β-$LnYbSe_3$ (Ln = La, Ce, Pr, Nd, Sm), are black in color, as are the title compounds.[14] The UV−vis-NIR diffuse reflectance spectra (Figure 13) of $Ln_xLu_ySe_z$ (Ln = La, Ce, Pr, Nd, Sm, Gd) were collected, and the band gaps were extrapolated from the absorption edges.[39] For La_3LuSe_6, Ce_3LuSe_6, β-$PrLuSe_3$, β-$NdLuSe_3$, $Sm_{1.82}Lu_{2.18}Se_6$, and $Gd_{1.87}Lu_{2.13}Se_6$, the band gaps were found to be 1.26, 1.10, 1.56, 1.61, 1.51, and 1.56 eV, respectively. The more condensed structure that Ln_3LuSe_6 (Ln = La, Ce) adopts may be the reason for their considerably smaller band gaps compared to those of the Pr-, Nd-, Sm-, and Gd-containing phases. The smaller value for Ce_3LuSe_6 is the result of the relatively low energy of the $4f^1 \rightarrow 4f^05d^1$ transition for cerium. The fine-structure observed in the spectra for β-$PrLuSe_3$, β-$NdLuSe_3$, and $Sm_{1.82}Lu_{2.18}Se_6$ is actually caused by f−f transitions within the lanthanide ions. There is also pronounced tailing off of the transition observed for La_3LuSe_6 that could be attributed to an indirect band gap or to an impurity like Sb_2Se_3.[40]

Conclusions

Molten Sb_2Q_3 (Q = S, Se) fluxes have been proven themselves to be useful in the preparation of ternary and quaternary interlanthanide chalcogenides. The composition and structure of the products depends highly on the choices of lanthanides and chalcogenides. In this present study, we detailed the synthesis of lutetium-based interlanthanide selenides $Ln_xLu_ySe_z$ (Ln = La, Ce, Pr, Nd, Sm, Gd) using a Sb_2Se_3 flux. All of these compounds show diverse structures and physical properties as a function of the Ln ions. Magnetic measurements have shown that both β-$PrLuSe_3$ and β-$NdLuSe_3$ are Curie−Weiss-type paramagnets. $Sm_{1.82}Lu_{2.18}Se_6$ exhibits van Vleck paramagnetism. $Gd_{1.87}Lu_{2.13}Se_6$ was found

(39) Schevciw, O.; White, W. B. *Mater. Res. Bull.* **1983**, *18*, 1059.
(40) Sutorik, A. C.; Kanatzidis, M. G. *Chem. Mater.* **1997**, *9*, 387.

to have an antiferromagnetic transition around 4 K, whereas Ce_3LuSe_6 has soft ferromagnetic ordering below 5 K.

Acknowledgment. This work was supported by the U.S. Department of Energy under Grant DE-FG02-02ER45963 through the EPSCoR Program. Funds for the purchase of the UV−vis-NIR spectrometer used in these studies were provided through the Chemical Sciences, Geosciences and Biosciences Division, Office of Basic Energy Sciences, Office of Science, Heavy Elements Program, U.S. Department of Energy under Grant DE-FG02-01ER15187. J.S.B. and E.S.C. acknowledge support from NSF-DMR 0203532. A portion of this work was performed at the National High Magnetic Field Laboratory, which is supported by the National Science Foundation Cooperative Agreement No. DMR-0084173, by the State of Florida, and by the Department of Energy.

Supporting Information Available: X-ray crystallographic files in CIF format for Ln_3LuSe_6 (Ln = La, Ce), β-$LnLuSe_3$ (Ln = Pr, Nd), and $Ln_xLu_{4-x}Se_6$ (Ln = Sm, Gd; x = 1.82, 1.87), selected bond distances for Ln_3LuSe_6 (Ln = La, Ce), β-$LnLuSe_3$ (Ln = Pr, Nd), and $Ln_xLu_{4-x}Se_6$ (Ln = Sm, Gd; x = 1.82, 1.87) (Tables S1, S2, and S3), and magnetization data for β-$LnLuSe_3$ (Ln = Pr, Nd) and $Sm_{1.82}Lu_{2.18}Se_6$. This material is available free of charge via the Internet at http://pubs.acs.org.

IC701012J